# INVESTIGATION OF ROTOR NOISE PREDICTION USING DIFFERENT AEROACOUSTIC METHODS IN TIME DOMAIN

**Han Zhonghua*, Song Wenping*, Qiao Zhide***
***Northwestern Polytechnical University, Xi'an, 710072, P.R.China**

**Keywords**: *helicopter rotors, acoustic noise, unsteady flow, Ffowcs Williams-Hawking equation, Kirchhoff method*

## Abstract

*In this study, the aeroacoustic-noise field generated by transonic rotors in hover and forward flight was calculated using Kirchhoff method and revised FW-H (Ffowcs Williams-Hawkings) method with a penetrable surface. The noise aerodynamically generated by rotating blades was taken as an equal to the acoustic radiation from a moving surface entirely surrounding the blades. To obtain the nonlinear near-field noise signal, the 3-D unsteady Euler's equations were numerically solved using a central finite-volume scheme and a dual-time stepping method, and the aerodynamic data over integration surface were directly extracted from the Euler solutions. The far-field noise signal was calculated by performing the integral of different acoustic formulas, with the source terms evaluated at the emission time. The comparison of computed results with experimental data was made and reasonably good agreement was achieved. It was also shown that Kirchhoff method and revised FW-H method are accurate and efficient for predicting quadrupole noise of transonic rotors, and that the revised FW-H method is more reliable than Kirchhoff method for the different choices of rotating integration surface.*

## 1 Introduction

In addition to high aerodynamic performance, low-noise radiation has also been taken one of the most important design criterions for the design of modern helicopter rotors. To reduce the aeroacoustic noise by caRefully designing the helicopter rotors, accurate and reliable noise-prediction tools should be available to provide necessary guidance for helicopter designers. Over the past decades, great progress has been made both in modeling the aerodynamically generated sound, and in developing the accurate prediction methods in time domain.

The FW-H equation [1], which was a rearrangement of Navier-Stokes equations, provided an accurate theoretical model for describing the noise propagation from a moving surface to far field. The Farassat1A method, solving the linear part of FW-H equation, has been successfully applied in linear-noise prediction [2] for more than 20 years. The method of solving FW-H equation predicts linear noise quite well, but it would run into complication when predicting nonlinear quadruple noise as the integration surface is the blade itself and nonlinear effects are not included in surface integral.

To calculate the nonlinear noise, e.g. transonic Impulsive (HSI) noise, Farassat and Mayers [3] proposed a general Kirchhoff formulation. This integration surface of Kirchhoff formulation is fictitious and penetrable. The main benefit of this method is that the nonlinear effect can be accounted for by surface integral, with surface surrounding the nonlinear flow region. With the maturation of computational fluid dynamics (CFD), the three-dimensional unsteady flow field of helicopter rotors can be numerically simulated by solving Euler' equations or Navier-Stokes equations. The near-field noise can be directly obtained from these unsteady solutions. But it's not practical to predict the far-field noise by CFD calculations due to the excessive computational

costs and strong numerical dissipation. Kirchhoff method, coupled with the near-field CFD solution, has been proved to be efficient for predicting impulsive noise. More recently, a form of FW-H equation applied for a permeable surface was proposed to improve the efficiency of quadrupole-noise prediction [4]. The calculation practices for hover rotors showed preliminarily that this revised FW-H method gained the same befit as the Kirchhoff method when predicting transonic noise [5-6].

The main purpose of this paper was to explore an accurate, efficient and reliable time-domain method for predicting the noise generated by transonic rotors both in hover and in forward flight. The focus of this paper will be on the prediction of HSI noise. However, the presented methods were readily applicable to Blade-vortex Interaction (BVI) noise as well if the flow-field calculation was replaced by high-resolution method. The research results and the developed code were expected to be useful to the aerodynamics-aeronautics integration design of helicopter rotors.

## 2 Aerodynamic Methods

The flow fields around the transonic helicopter rotors in hover and in forward flight were numerically simulated by solving three-dimensional unsteady Euler's equations. And an algebraic method based on transfinite-interpolation theory [7] was employed to quickly generate the O-H type algebraic grid around single rotor blade (See Fig.1).

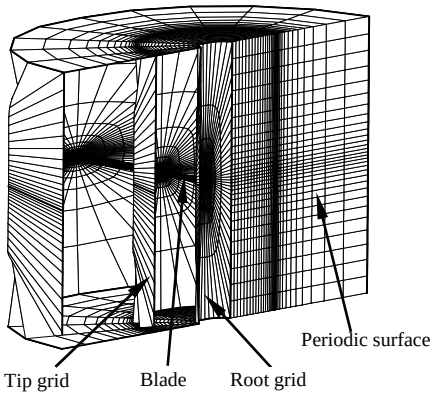


Fig.1 Schematics for grid of single blade

### 2.1 Hovering flow simulation

To numerically simulate the quasi-steady flow around rotor in hover, 3-D unsteady Euler's equations for an inertial coordinate system were projected to a blade-fixed coordinate system, while the values of all the physical variables were kept to be absolute. Assuming that the angular velocity of rotors is

$$\vec{\omega} = (0, \omega, 0)^T \tag{1}$$

Then the governing equations for hover rotors flow can be written as:

$$\frac{\partial}{\partial t}\iiint_V \vec{\mathbf{W}} dV + \iint_S (\overline{\overline{\mathbf{F}^1}} - \overline{\overline{\mathbf{F}^2}}) \cdot \vec{\mathbf{n}} dS + \iiint_V \vec{\mathbf{G}} \cdot \vec{\mathbf{n}} dV = 0 \tag{2}$$

Where

$$\vec{\mathbf{W}} = \begin{bmatrix} \rho \\ \rho u \\ \rho v \\ \rho w \\ \rho E \end{bmatrix} \quad \overline{\overline{\mathbf{F}^1}} = \begin{bmatrix} \rho\vec{\mathbf{q}} \\ \rho u\vec{\mathbf{q}} + p\vec{\mathbf{i}}_x \\ \rho v\vec{\mathbf{q}} + p\vec{\mathbf{i}}_y \\ \rho w\vec{\mathbf{q}} + p\vec{\mathbf{i}}_z \\ \rho H\vec{\mathbf{q}} \end{bmatrix}, \overline{\overline{\mathbf{F}^2}} = \begin{bmatrix} \rho\vec{\mathbf{q}}_b \\ \rho u\vec{\mathbf{q}}_b \\ \rho v\vec{\mathbf{q}}_b \\ \rho w\vec{\mathbf{q}}_b \\ \rho E\vec{\mathbf{q}}_b \end{bmatrix}$$

$$\vec{\mathbf{G}} = \begin{bmatrix} 0 \\ \rho\omega w \\ 0 \\ -\rho\omega u \\ 0 \end{bmatrix}, \vec{\mathbf{q}} = u\vec{\mathbf{i}}_x + v\vec{\mathbf{i}}_y + w\vec{\mathbf{i}}_z, \vec{\mathbf{q}}_b = \vec{\omega} \times \vec{\mathbf{r}} \tag{3}$$

In equation (3), $\rho, u, v, w, p, E, H$ denote density, velocity in x-direction, velocity in y-direction, velocity in z-direction, pressure, total energy, and total enthalpy, respectively.

A central finite-volume method and a 5-stages explicit Runge-Kutta scheme [8] were used in this study, and the quasi-steady solution procedure of equation (2) was fairly similar to a steady calculation of Euler's equations.

### 2.2 Forward flight flow simulation

According to Ref.9, the 3-D Euler's equations governing the flow around rotor blades in arbitrary motion can be written as

$$\frac{D}{Dt}\iiint_V \vec{\mathbf{W}} dV + \iint_S \overline{\overline{\mathbf{F}'}} \cdot \vec{\mathbf{n}} dS = 0 \tag{4}$$

Where

$$\overline{\overline{\mathbf{F}'}} = \begin{bmatrix} \rho(\vec{\mathbf{q}} - \vec{\mathbf{q}}_b) \\ \rho u(\vec{\mathbf{q}} - \vec{\mathbf{q}}_b) + p\vec{\mathbf{i}}_x \\ \rho v(\vec{\mathbf{q}} - \vec{\mathbf{q}}_b) + p\vec{\mathbf{i}}_y \\ \rho w(\vec{\mathbf{q}} - \vec{\mathbf{q}}_b) + p\vec{\mathbf{i}}_z \\ \rho H(\vec{\mathbf{q}} - \vec{\mathbf{q}}_b) + p\vec{\mathbf{q}}_b \end{bmatrix} \tag{5}$$

In equation (5), $\vec{\mathbf{q}}_b$ denotes the velocity of the boundary of arbitrary control volume. The motion effect of grid cells (embodied by $\vec{\mathbf{q}}_b$) was introduced into the flux terms of governing equations. This treatment gained the benefit that no source terms occur on the right-hand side of the equations. Hence, the calculation was expected to be simplified to some extent.

In current practice, a method of deformable-grid developed by Ref.10 was applied to the forward-flight simulation. A multiple-block grid was generated to cover the entire rotor, with each grid block covering a blade and adjacent to the two neighboring blocks. The entire grid system moved together with the rotor blades and the grid cells were deformable considering the pitching and flapping motion of rigid blades.

To obtain the time-accurate solution of forward flight flows, a "dual-time stepping method" [9] was used together with a cell-centered finite-volume scheme and an explicit Runge-Kutta method.

The near-field aeroacoustic noise was directly extracted from the unsteady CFD solutions obtained by solving 3-D unsteady Euler's equations. Based on the near-field aerodynamic data, the far-field acoustic noise was calculated using the aeroacoustic methods that would be described in the following section.

## 3 Acoustic Methods

Time-domain methods, compared to frequency-domain methods, are more appropriate for numerical implementation of predicting the aeroacoustic noise. According to the authors' understanding, these time-domain methods can be classified into two types, namely Kirchhoff method solving the general wave equation and FW-H method solving Ffowcs Williams-Hawkings equation. FW-H method mainly includes Farassat 1A method for linear-noise prediction and a revised method for transonic noise prediction. Kirchhoff method and FW-H method were both used and validated in prediction of the complex acoustic field generated by transonic helicopter rotors. This section described the time-domain integral methods used in the study.

### 3.1 Kirchhoff Method

Kirchhoff formulation was originally used to describe the diffraction of light, and was extended to solve the problem of acoustic field. In 1988, Farassat and Myers derived the general form of Kirchhoff formulation by use of general -function theory [3].Then Kirchhoff Method was successfully used in prediction of HSI noise generated by transonic rotors.

Consider a piece-wise smooth surface defined by $f(\vec{\mathbf{x}},t)=0$, which surrounds rotor blade or other types of wall boundary, arbitrarily moving in a stationary fluid. Assuming that $\nabla f=\vec{\mathbf{n}}$ and $\partial f/\partial t=-v_n$ ($\vec{\mathbf{n}}$ is the unit normal outer vector and $\vec{\mathbf{v}}$ is the velocity vector of control surface), then by use of general function theory, the general wave equation (or Kirchhoff equation) [3] can be written as

$$\left(\frac{1}{c_0^2}\frac{\bar{\partial}^2}{\partial t^2}-\frac{\bar{\partial}^2}{\partial x_i^{\,2}}\right)p'(\vec{\mathbf{x}},t)=-\left(p_n'+\frac{1}{c_0}M_n\dot{p}'\right)\delta(f)-\frac{1}{c_0}\frac{\bar{\partial}}{\partial t}[M_n p'\delta(f)]-\frac{\bar{\partial}}{\partial x_i}[p_n'\delta(f)] \tag{6}$$

Where $\frac{1}{c_0^2}\frac{\partial^2}{\partial t^2}-\frac{\partial^2}{\partial x_i^2}$ is the wave arithmetic operators; $p'(\vec{\mathbf{x}},t)$ denotes the acoustic pressure of time $t$ for a observing point (coordinate vector is $\vec{\mathbf{x}}$) outside the surface $f=0$ and note that $p'=p-p_\infty$; $c_0$ is speed of sound (assuming that it is a constant for linear wave propagation); $\delta(f)$ is Dirac function; the bar over the derivative operators denotes the generalized differentiation and a dot over a symbol denotes the derivative with respect to the source time. Besides, one has

$$p_n'=\frac{\partial p'}{\partial \mathbf{x}_i}\cdot\mathbf{n}_i,\mathbf{M}_i=\frac{\mathbf{v}_i}{c_0},M_n=\mathbf{M}_i\cdot\mathbf{n}_i \tag{7}$$

According to Farassat and Myers's derivation, a solution of equation (6) named Kirchhoff formulation can be written as

$$p'(\vec{\mathbf{x}},t)=\frac{1}{4\pi}\iint_S\left[\frac{E_1}{r(1-M_r)}+\frac{E_2p'}{r^2(1-M_r)}\right]_{ret}\cdot dS \tag{8}$$

Where, $E_1$ and $E_2$ are defined as follows:

$$
\begin{aligned}
E_1 &= M_n p'_M - p'_n - \frac{M_n \dot{p}'}{c_0} \\
&\quad + \frac{(\dot{n}_r - \dot{M}_n - \dot{n}_M) p' + (\cos\theta - M_n)\dot{p}'}{c_0(1-M_r)} \\
&\quad + \frac{\dot{M}_r(\cos\theta - M_n)p'}{c_0(1-M_r)^2} \\
E_2 &= \frac{1-M^2}{(1-M_r)^2}(\cos\theta - M_n)
\end{aligned} \tag{9}
$$

Where subscript "ret" denotes restarted time (or emission time) and $\mathbf{r}_i$ is radius vector. Furthermore, one has

$$
\begin{aligned}
&p'_M = \frac{\partial p'}{\partial x_i}\cdot \mathbf{M}_i, M_r = \mathbf{M}_i \cdot \mathbf{r}_i / r \quad M_n = \mathbf{M}_i \cdot \mathbf{n}_i, \cos\theta = \mathbf{n}_i \cdot \mathbf{r}_i / r \\
&\dot{M}_n = \dot{\mathbf{M}}_i \cdot \mathbf{n}_i, \dot{M}_r = \dot{\mathbf{M}}_i \cdot \mathbf{r}_i / r, \dot{n}_M = \dot{\mathbf{n}}_i \cdot \mathbf{M}_i, \dot{n}_r = \dot{\mathbf{n}}_i \cdot \mathbf{r}_i / r
\end{aligned} \tag{10}
$$

The integration surface of Kirchhoff formulation is assumed to be a fictitious penetrable surface that allows the fluid flow through. With integration surface surrounding the nonlinear flow region， Kirchhoff method gains the benefit that nonlinear effect can be accounted for by surface integral. Coupled with modern CFD simulation techniques, Kirchhoff method was capable of predicting transonic rotor noise (especially HSI noise).

## 3.2 FW-H Method

### *3.2.1 FW-H equation*

In theory, Navier-Stokes equations in fluid dynamics can describe the problem of aeroacoustic-noise generation. And FW-H equation is just an exact rearrangement of N-S equations into the form of an inhomogeneous wave equation. Hence FW-H equation, the most general form of the Lighthill acoustic analogy, has been taken as one of the most important theoretical foundations for rotor aeroacoustics.

In 1969, Ffowcs Williams and Hawkings [1] rearranged the Navier-Stokes equation to an inhomogeneous wave equation (namely FW-H equation) by using general function theory. Consider a control surface $f(\bar{\mathbf{x}},t)=0$ moving in a stationary fluid. The FW-H equation derived by Ffowcs Williams and Hawkings can be written as

$$
\begin{aligned}
(\frac{1}{c^2}\frac{\partial^2}{\partial t^2} - \frac{\partial^2}{\partial \mathbf{x}_i^2}) p'(\bar{\mathbf{x}},t) &= \frac{\bar{\partial}}{\partial t}\{[(\rho_0 v_n + \rho(u_n - v_n)]\delta(f)\} \\
&\quad - \frac{\bar{\partial}}{\partial \mathbf{x}_i}\{[-\mathbf{P}'_{ij}\cdot \mathbf{n}_j + \rho \mathbf{u}_i(u_n - v_n)]\delta(f)\} \\
&\quad + \frac{\bar{\partial}^2}{\partial \mathbf{x}_i \mathbf{x}_j}[\mathbf{T}_{ij} H(f)]
\end{aligned} \tag{11}
$$

Where, $\rho, u_i, P_{ij}$ denotes density, tensors of velocity and stress, respectively; $T_{ij} = -P'_{ij} + \rho u_i u_j - c^2 \rho' \delta_{ij}$ is Lighthill stress tensor and $\delta_{ij}$ is Kronecker delta ； Subscript " 0 "indicates the free-stream undisturbed quantities, and superscript "′" denotes the disturbed values; $H(f)$ is Heaviside function and $\delta(f)$ is Dirac function which satisfies $H(f) = \begin{cases} 1 & f(\bar{\mathbf{x}},t) > 0 \\ 0 & f(\bar{\mathbf{x}},t) < 0 \end{cases}$ and $\delta(f) = \frac{\bar{\partial} H(f)}{\partial f}$.

Provided that the moving surface $f(\bar{\mathbf{x}},t)=0$ is coincident with the rotor-blade surface, the solid-boundary condition $u_n = v_n$ can be applied to equation (11), which yields the most popular form of FW-H equation:

$$
(\frac{1}{c^2}\frac{\partial^2}{\partial t^2} - \frac{\partial^2}{\partial \mathbf{x}_i^2}) p'(\bar{\mathbf{x}},t) = \frac{\bar{\partial}}{\partial t}[(\rho_0 v_n)\delta(f)] - \frac{\bar{\partial}}{\partial \mathbf{x}_i}[\mathbf{l}_i \delta(f)] + \frac{\bar{\partial}^2}{\partial \mathbf{x}_i \mathbf{x}_j}[\mathbf{T}_{ij} H(f)] \tag{12}
$$

Where, $\mathbf{l}_i = -\mathbf{P}'_{ij}\cdot \mathbf{n}_j$. The three source terms of the right-hand side of the Equation (12) are known as monopole (or thickness), dipole (or loading) and quadrupole source terms, respectively. From equation (12), one can immediately get two conclusions: 1) thickness noise and loading noise are surface source (determined by Dirac function) and quadrupole noise is volume source (determined by Heaviside function); 2) the thickness noise and loading noise are linear and quadrupole noise is nonlinear.

FW-H equation provides the exact governing equation of acoustic field generated by a solid-body boundary in arbitrary motion. Finding the methods to solve FW-H equation is particularly important both in theory and for engineering application to helicopter rotors.

### *3.2.2 Farassat Method*

Starting from equation (12), Farassat (See Ref.2) derived the solutions of the liner parts of FW-H equation by use of 3-D free-space Green's

function, namely Farassat 1 and Farassat 1A formulation. It was proved by practices that Farassat 1A was more suitable for numerical calculation than Farassat 1. In this paper, Farassat 1A was used to quantitatively predict the linear noise (namely thickness noise and loading noise) of transonic rotors. According to Farassat1A formula, the acoustic pressure of an observing point off the blade can be written as

$$\begin{aligned} p'_T(\bar{\mathbf{x}},t) &= \frac{1}{4\pi}\int_{f=0}\left[\frac{\rho_0 c_0(\dot{M}_n+\dot{n}_M)}{r(1-M_r)^2}\right]_{ret} dS \\ &+\frac{1}{4\pi}\int_{f=0}\left[\frac{\rho_0 c_0 M_n \dot{M}_r}{r(1-M_r)^3}\right]_{ret} dS \\ &+\frac{1}{4\pi}\int_{f=0}\left[\frac{\rho_0 c_0^2 M_n(M_r-M^2)}{r^2(1-M_r)^3}\right]_{ret} dS \end{aligned} \qquad (13)$$

$$\begin{aligned} p'_L(\bar{\mathbf{x}},t) &= \frac{1}{4\pi}\int_{f=0}\left[\frac{\dot{l}_r}{c_0 r(1-M_r)^2}\right]_{ret} dS \\ &+\frac{1}{4\pi}\int_{f=0}\left[\frac{l_r-l_M}{r^2(1-M_r)^2}\right]_{ret} dS \\ &+\frac{1}{4\pi}\int_{f=0}\left[\frac{l_r\dot{M}_r}{c_0 r(1-M_r)^3}\right]_{ret} dS \\ &+\frac{1}{4\pi}\int_{f=0}\left[\frac{l_r(M_r-M^2)}{r^2(1-M_r)^3}\right]_{ret} dS \end{aligned} \qquad (14)$$

Where, subscript "T" and "L" denote thickness noise and loading noise, respectively and

$$l_r = \mathbf{l}_i\cdot\mathbf{r}_i/r \quad l_M = \mathbf{l}_i\cdot\mathbf{M}_i, \dot{l}_r = \dot{\mathbf{l}}_i\cdot\mathbf{r}_i/r \qquad (15)$$

By performing the integration of equation (13-14) on the blade surface, the thickness and loading noise for a given helicopter rotor can be easily specified if the motion property and the surface-pressure distribution are known. Over the past two decades, Farassat1A formula was successfully widely used in predicting the near-field and far-field noise of subsonic rotors. And in our opinion, it was Farassat' outstanding works that made the time-domain method of solving FW-H equation become applicable. However, when the flow filed around the rotor blades becomes transonic and the non-linear effect becomes apparent, the quadruple source can not be reasonably neglected, which leads to the difficulty of the excessive computing incurred by the volume integration of quadrupole source.

### *3.2.3 A Revised FW-H Method*

For many years, the FW-H equation has been used in applications assuming that the control surface $f=0$ is coincident with the blade surface. In fact, Ffcows himself proposed [4] to a form of FW-H applied to a penetrable moving surface (Just as equation (11)). When the surface is located off the blade and surrounds the nonlinear flow region, the nonlinear effect of flow inside the surface can be accounted for by the surface noise source. This academic thought gave a motivation to explore a form of solution of FW-H equation that can be used just as Kirchhoff method and it was recently firstly implemented by di Francescantonio, and further better used by Brentner and Farassat both in theoretical understanding and in engineering application. (See Ref.6).

According to Brentner and Farassat's derivation, when integration surface is located in the linear flow region, FW-H equation is equal to Kirchhoff equation. This conclusion provided the analytical base for using the solution of FW-H equation just as Kirchhoff method. Assuming that

$$\begin{aligned} \mathbf{U}_i &= (1-\frac{\rho}{\rho_0})\mathbf{v}_i + \frac{\rho\mathbf{u}_i}{\rho_0} \\ \mathbf{L}_i &= -\mathbf{P}'_{ij}\cdot\mathbf{n}_j + \rho\mathbf{u}_i(u_n-v_n) \end{aligned} \qquad (16)$$

Then the form of FW-H equation applied to a fictitious penetrable moving surface can be written as

$$\begin{aligned} (\frac{\partial^2}{c^2\partial t^2}-\frac{\partial^2}{\partial\mathbf{x}_i^2})p'(\bar{\mathbf{x}},t) &= \frac{\bar{\partial}}{\partial t}[\rho_0 U_n\delta(f)] \\ &-\frac{\bar{\partial}}{\partial\mathbf{x}_i}[\mathbf{L}_i\delta(f)]+\frac{\bar{\partial}^2}{\partial\mathbf{x}_i\mathbf{x}_j}[\mathbf{T}_{ij}H(f)] \end{aligned} \qquad (17)$$

The above form is very similar to equation (12), hence, one can immediately write out the solution according to Farassat 1A formulation (equation (13-14)). But the solution no longer has the same physical meaning as thickness and dipole noise. For concision, the solution of equation (17) was not listed here. Note that if $f=0$ of FW-H equation was reverted to the blade surface itself, the revised solution will be identical to Farassat 1A formula and have apparent physical meaning.

If the solution of equation (17) is utilized just like Kirchhoff method, one can gain the

same benefit as equation (8). This revised FW-H method can predict quadrupole noise by surface integration. If the surface $f=0$ is located adequately far away from the blade and entirely surrounding the non-linear flow region, the third term in equation (17) can be reasonably neglected, theRefore, the efficiency of predicting the noise for the complicated, nonlinear acoustic resource could be substantially improved.

In current practice, the Farassat 1A formula was used to quantitatively predict the thickness and loading noise of transonic helicopter rotors. This treatment was useful for guiding the acoustic design of transonic rotors because of the apparent physical meaning of the solutions. The Kirchhoff method and revised FW-H method were both used to predict the total acoustic noise, including quadrupole noise. Subtracting thickness and loading noise from the total noise, the value of quadrupole noise was specified. Coupling the time-domain method of section 3 with CFD techniques of section 2, a noise-predicting methodology and a computer code for transonic helicopter rotor was developed and was ready to be used for aerodynamics-aeronautics integration design.

## 4 Results and Discussing

This section firstly described two vital points for noise prediction of this paper: the choice of integration surface and the solution of retarded time. Then, the numerical examples of helicopter rotors in hover and in forward flight were presented and analyzed.

### 4.1 Choices of Integration Surface and Solution of Retarded-time Equation

To perform the integration of time-domain integral method, an appropriate integration surface should be caRefully selected, and this selection may have significant influence on the computed results. There are two types of integration surfaces that were generally used in rotor noise prediction, namely rotating surface and non-rotating surface. Both of them were used in this study. The rotating surface was selected as some surfaces of CFD grid that have the same angular velocity of the rotors. One of the main advantages of rotating surface is that the aerodynamic data on integration surface can be directly obtained from CFD solutions avoid the numerical error caused by interpolation. The non-rotating surface was defined as a cylindrical surface that was relatively stationary with respect to blade hub. This surface was divided into elements along its circular and axial direction. To quickly obtain the aerodynamic data of these grid cells, a 3-D linear interpolation was pReformed from CFD solutions. And a fast searching methodology based “inverse map” was used to improved the efficiency of searching the contribution CFD grid cell for a considering point. It was shown by the following numerical examples that the accuracy of the interpolation method was acceptable for the final results.

Another key point of this implementation was the solution of retarded-time equation. Assuming that a source over the integration surface rotates with angular velocity $(0,\omega,0)^T$ and moves forward with a velocity $\vec{\mathbf{v}}_\infty$, then the retarded time for a given observing point (moving also with $\vec{\mathbf{v}}_\infty$) can be written as

$$\tau = t - \frac{1}{c_0}\left| \vec{\mathbf{x}}_0 - \begin{bmatrix} \cos(\omega\tau) & 0 & -\sin(\omega\tau) \\ 0 & 1 & 0 \\ \sin(\omega\tau) & 0 & \cos(\omega\tau) \end{bmatrix} \vec{\mathbf{y}}_0 + \vec{\mathbf{v}}_\infty (t-\tau) \right| \quad (18)$$

Where, $\tau$ is the retarded time, and $\vec{\mathbf{x}}_0$, $\vec{\mathbf{y}}_0$ denote the coordinate vectors of the observing and the source point at zero time, respectively. Equation (18) is called retarded-time equation. Since the solution of this equation can not be explicitly deduced, a solution method base on simple-iteration technique, in this paper, was developed and a good convergence was achieved. No matter that the integration surface is rotating or non-rotating one, the same solving procedure was conducted for rotor both in hover and forward flight, which was helpful for integrating the noise-prediction methods into a single computer code for different flight conditions and different types of integration surface.

### 4.2 Hovering rotor example

To validate the computational results for transonic hover rotor, an UH-1H model was adopted (Note that the main non-linear noise for this case is HSI noise). UH-1H rotor is a one-seventh scale two-bladed model with untwisted rectangular-platform blades and NACA0012 airfoil section. The aspect ration is 13.71 and chord length is 0.0762m.The observing microphone is located 3.09R away from the rotating axis(R is the radius of rotor, See fig.2). The experimental data was presented by Boxwell in Ref.11. The hover rotor simulation was conducted on a computational grid with $101\times31\times61$ points ( $31$ points on the blade). The non-rotational surface was divided into $360\times30$ surface elements ( $360$ segments along the circular direction and $30$ segments along the axial direction).

Fig.3 presents the comparison of computed results and experimental data with a blade-tip Mach number $M_{tip}=0.85$ .The integration surface for Farassat 1A method was the blade-surface grid and the surface for Kirchhoff and revised FW-H method was the combination of grid surfaces J=20 and K=40 of computational grid. Thickness noise and loading noise predicted by Farassat 1A method was clearly indicated in fig.2, which showed that the thickness noise was the main source as the test case was conducted in non-lift mode. The difference of results between Farassat 1A and other two methods (Kirchhoff and revised FW-H method) denoted the value of the non-linear quadrupole noise generated by transonic rotor. And result of revised FW-H method showed slightly better agreement with the experimental data.

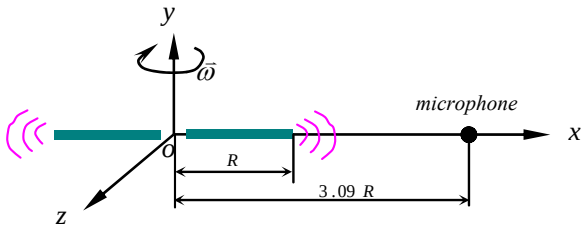


Fig. 2 Schematics of the observing microphone location for UH-1H rotor in hover

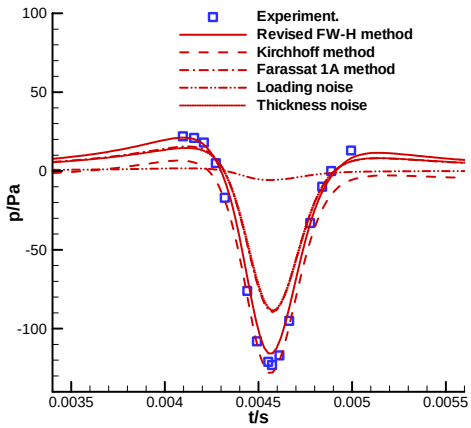


Fig.3 Comparison of the predicted noise of different methods using rotating surface for UH-1H hover rotor, $M_{tip}=0.85$ .

The comparison in Fig.4 was made to check the performance of Kirchhoff method and FW-H method when applied to a non-rotating surface. The integral circular cylinder was located 1.1R from the rotating axis. The time derivatives of flow variables were discretized by a 3-order finite difference. The computed results of two methods were both in good agreement with the experimental data, which showed the capability of in transonic-HSI-noise prediction.

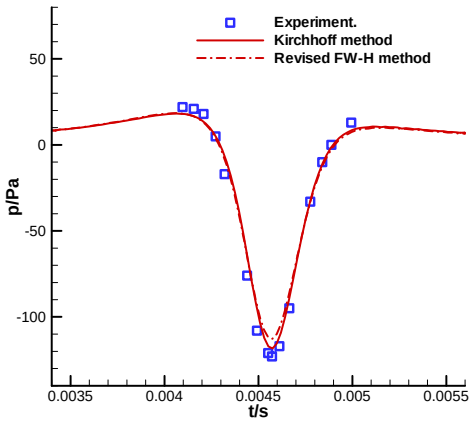


Fig.4 Comparison of the predicted noise of Kirchhoff and revised FW-H method using non-rotating surface for UH-1H hover rotor, $M_{tip}=0.85$ .

The purpose of Fig.5 was to verify the perdition performance of Kirchhoff method revised FW-H method for different locations of rotating surface, with a transonic tip Mach number $M_{tip}=0.90$ . Surface 1-3, illustrated in Fig.5a, is coincident with grid surfaces J=5, J=10 and J=20, respectively.

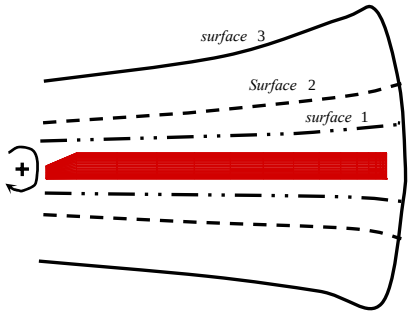


Fig.5a Schematics of different locations of rotating surface

As illustrated in Fig.5b, substantial error was caused by Kirchhoff method, when rotating surface was located in nonlinear flow region of the rotor blade. This can be interpreted by the essence that the governing equation of Kirchhoff method is linear wave equation. By contrast with Kirchhoff method, revised FW-H method showed better robustness (See Fig.5c) as it is the exact rearrangement of Navier-Stokes equation. As integration surface close to rotor blade (e.g. surface 1), the less nonlinear flow was surrounded, hence, the predicted results showed relatively greater difference from experimental data, and when the integration surface was far away from rotor blade (e.g. surface 3), the computed result showed relatively good agreement with experimental data, as illustrated in Fig.5c. It can be also reasoned that the computed result of revised FW-H method would be the same as that of Farassat 1A method if the rotating surface was coincident with the blade surface grid.

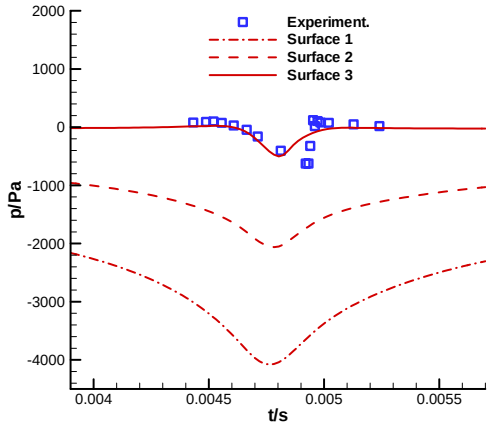


Fig.5b Comparison of the predicted result of Kirchhoff method applied to different rotating surfaces for UH-1H hover rotor, $M_{tip} = 0.90$ .

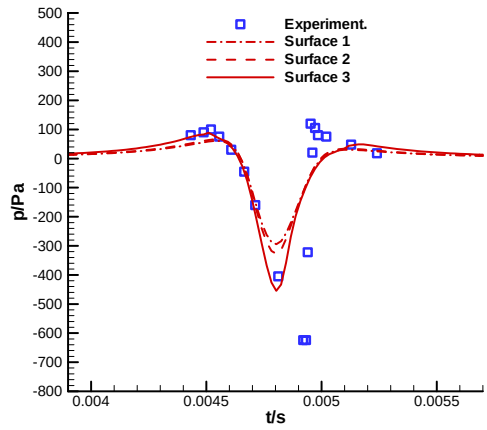


Fig.5c Comparison of the predicted result of revised FW-H method applied to different rotating surfaces for UH-1H hover rotor, $M_{tip} = 0.90$ .

The influence of the discrete accuracy for time derivatives of flow variable on the non-rotating surface was investigated in Fig.6 for a transonic tip Mach number 0.95. In Fig.6a and Fig.6b, it was shown that revised FW-H method was more sensible than Kirchhoff method for different discrete accuracy. This may be explained as: revised FW-H method deals with more time derivatives than Kirchhoff method, and much error must be introduced by numerical discretization. It can be concluded by this study that 2-order accuracy was adequately appropriate for Kirchhoff method, while 3-order or higher discrete accuracy should be conducted for revised FW-H method.

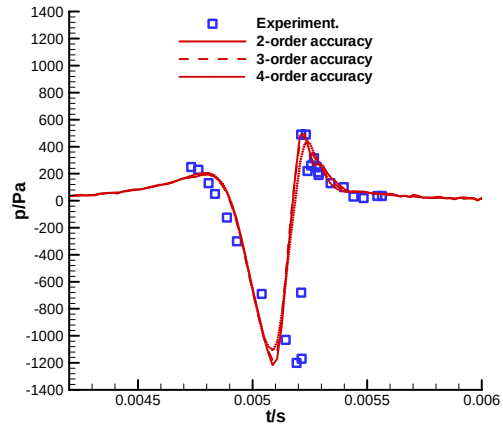


Fig.6a Comparison of predicted results of Kirchhoff method by 2 to 4 order discrete accuracy of time derivatives.

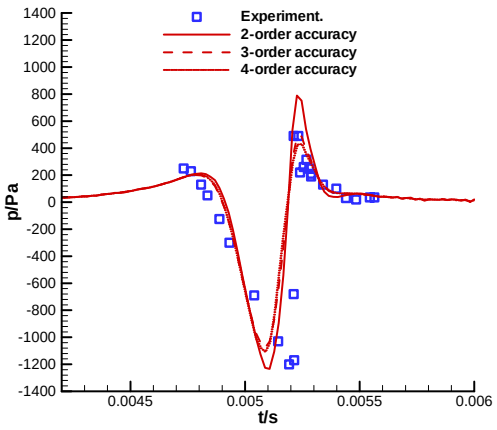


Fig.6b Comparison of predicted results of revised FW-H method by 2 to 4 order discrete accuracy of time derivatives.

## 4.3 Forward Flight example

An AH-1/OLS rotor was adopted to validate the computed results for transonic rotor in forward flight. AH-1/OLS is a one-seventh two-bladed model with rectangular-platform blades and OLS airfoil section. The blades linearly twist with angle of $-10^0$. The aspect ratio is 9.22 and the chord length is 0.1039m. The location of the observing microphone was illustrated in Fig.7. A transonic operation condition was adopted with rotating tip Mach number $M_{\omega R}=0.666$, an advancing ratio $\mu=0.345$ and a tilting angle of blade plane $\alpha_T=-3.0^0$. The periodic pitching motion of blades is give by

$$\theta=8.20^0+1.17^0\cos(\psi)-10.67^0\sin(\psi) \qquad (19)$$

Where, $\Psi$ is the azimuthal angle of the rotor. The experimental data can be found in Ref.12. The unsteady simulation was conducted on a computational grid with $101\times31\times61$ points ($31$ points on the blade) for a single-blade block. The grid cells on the non-rotational integration surface were divided as $360\times30$ ($360$ segments along the circular direction and $30$ segments along the axial direction)

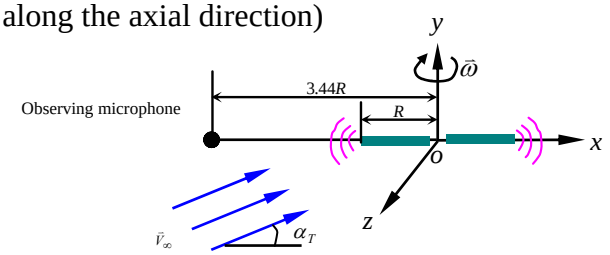


Fig.7 Schematics of observing microphone location for AH-1/OLS rotor in forward flight.

Fig.8 presents the comparison of computed results with experimental data using different methods using rotating surface. From this figure, the thickness, loading and quadrupole noise can be assessed, and the capability of Kirchhoff and revised FW-H method for predicting quadrupole noise was validated. Note that the computed negative-pressure-peak value was lower than the experimental data due to the numerical error caused by CFD simulation and the neglect of viscous effect.

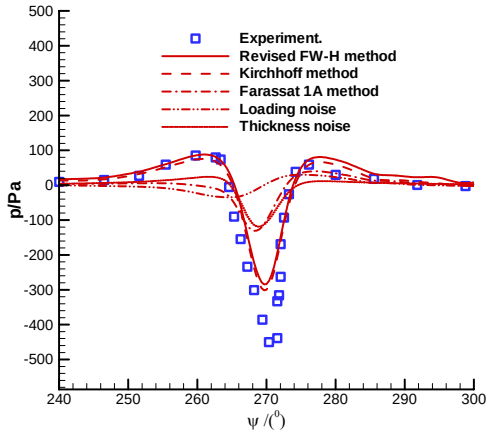


Fig.8 Comparison of the predicted result of different methods using rotating surface for AH-1/OLS rotor in forward flight, $M_{\omega R}=0.666$, $\mu=0.345$.

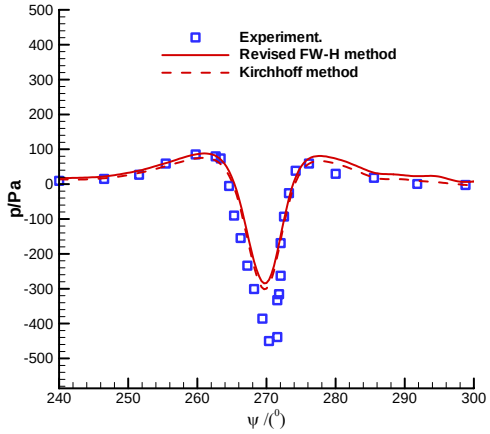


Fig.9 Comparison of the predicted noise of Kirchhoff and revised FW-H method using non-rotating surface for AH-1/OLS rotor in forward flight, $M_{\omega R}=0.666$, $\mu=0.345$.

Fig.9 illustrates the comparison of Kirchhoff and revised FW-H method using non-rotating surface. The integral circular cylinder was located 1.1R from the rotating axis. From Fig.9, the discretization of time derivatives of flow variables was conducted by a 3-order finite

difference. It was shown that the results of these two methods were both in reasonably good agreement with experimental data.

## 5 Conclusions

Coupling 3-D Euler flow solver and two types of time-domain acoustic method, an efficient and accurate methodology for aeroacoustic-noise prediction of transonic helicopter rotors in hover and forward flight was developed. The thickness noise and loading noise was predicted by Farassat 1A method, and the total noise was predicted by Kirchhoff method and a revised FW-H method, including the contribution of non-linear quadrupole noise. The developed code integrated the hover and forward flight flow simulation as well as different time-domain integral methods with both rotating and non-rotating integration surfaces. From the study practice, it could be concluded that revised FW-H method are more reliable than Kirchhoff method when applied to rotating surface, and it was suggested that Kirchhoff method is more appropriate for non-rotating surface and that 3-order or higher accuracy discretization for time derivatives on non-rotating surface used should be used in revised FW-H method.

## References


[1] Ffowcs Williams J.E., Hawkings D.L., Sound Generated by Turbulence and Surfaces in Arbitrary Motion. *Philosophical Transactions of the Royal Society*，Vol.A264, No.1151, pp 321-342, 1969.

[2] Farassat F., Linear Acoustic Formulas for Calculation of Rotating Blade Noise. AIAA Paper 83-0688, 1983.

[3] Farassat F., Myers M K. Extension of Kirchhoff's Formulation to Radiation from Moving Surface. *Journal of Sound and Vibration*, Vol.123, No.3, pp 451-460, 1988.

[4] Crighton, D.G., Dowling, A.P., Ffowcs Williams, J.E., Heckl, M., Leppington, F.G., *Modern Method in analytical Acoustics-Lecture Notes*, Spinger-verlag, 1992.

[5] di Francescantonio P. A., New Boundary Integral Formulation for the Prediction of Sound Radiation. Journal of Sound and Vibration, Vol. 202, No.4, pp 191-509, 1997.

[6] Brentner, K.S., Modeling Aerodynamically Generated Sound: Recent Advance in Rotor Noise Prediction, AIAA Paper 2000-0345, 2000.

[7] Rizzi, A., Eriksson, L.E., Transfinite Mesh Generation and Damped Euler Equation Algorithm for transonic Flow around Wing-Body Configuration. AIAA Paper 81-0999, 1981.

[8] Kroll, N., and Jain, R.K., Solution of Two-Dimensional Euler Equations Experience with a Finite Volume Code, DFVLR—FB, 87—41, 1987.

[9] Lin, C.Q., Pahlke, K., Numerical Solution of Euler Equations for Aerofoil in Arbitrary Motion, *Aeronautical Journal*, June/July, pp 207-214, 1994.

[10] Boniface J.-C., Sidès J., Mialon B. Numerical Simulation of Unsteady Euler Flow Around Multibladed Rotor in Forward Flight Using a Moving Grid Approach. *AHS, 51st Annual Forum and Display*, Fort Worth, TX (USA), 1995

[11] Boxwell, D.A., Yu, Y.H. and Schmitz, F.H., Hovering Impulsive Noise: Some Measured and Calculated Results. *Vertica*, Vol.3, pp.35-45, 1979.

[12] Kuntz M. Rotor Noise Prediction in Hover and Forward Flight Using Different Aeroacoustic Methods, AIAA Paper 96-1695,1996.